Surface & Coatings Technology 236 (2013) 518–524

Contents lists available at ScienceDirect

Surface & Coatings Technology

journal homepage: www.elsevier.com/locate/surfcoat

Preparation of the multifunctional antireflective films from a templating composite silica sol with entwining structures

Xiaoshan Meng, Yan Wang, Hongning Wang, Jing Zhong, Ruoyu Chen *

School of Petrochemical Engineering, Changzhou University, 1 Gehu Road, Changzhou, Jiangsu 213164, PR China

ARTICLE INFO

Article history:
Received 25 April 2013
Accepted in revised form 22 October 2013
Available online 30 October 2013

Keywords:
Silica antireflective films
Hydrophobicity
Hardness
Abrasion-resistance

ABSTRACT

Antireflective (AR) films were prepared by the sol–gel method and dip-coating process by using tetraethylorthosilicate (TEOS) as silica precursor. Silica nanoparticle (SiO_2-NP) sol was first synthesized via classical Stöber method, and then SiO_2-NPs in sol were chained in series by linear silicate polymers (SiO_2-LPs) to improve the film abrasion-resistant property. To further increase the transmittance of the SiO_2-LP/NP composite film, the template agent CTAB was introduced into the SiO_2-LP/NP composite sol. The experimental results revealed that the abrasion-resistant property had been enhanced with the increase of SiO_2-LPs addition and the pencil hardness of the composite film had reached 6H when the mole ratio of SiO_2-LPs to SiO_2-NPs was 0.7:1. Meanwhile, the transmittance was optimized when n_{CTAB}:n_{LPs} was equal to 0.15:1 in the composite sol, and at this mole ratio the average transmittance of the glass substrate coated with AR film was about 98.5% in the wavelength range of 400–800 nm, while that of the bare glass substrate was just 91.5%. Trimethylchlorosilane (TMCS) treatment was finally used to provide AR films with hydrophobicity. The water contact angle was significantly increased from 6° to 120° after TMCS treatment, affording the AR films excellent environmental resistance.

1. Introduction

To increase the transmittance of optical devices, AR films are always employed to reduce the optical loss, which is determined by the devices their own nature, to improve the practical performance of these devices, such as cathode ray tubes (CRT) [1], shielding windows [2], high-power lasers [3], solar collectors [4–6] and other applications [7]. As more attentions are paid to solar energy, the study of solar utilization rate has made an unceasing progress. The efficiency of solar collectors for the production of electricity depends primarily on the intensity of the incident sunlight. However, a basal drawback of any transparent cover materials that are used to create the vacuum for thermal insulation in concentrating solar power (CSP) systems is the reflection of the incident sunlight. Thus, the application of AR films is extraordinarily important to solar power plants. In consideration of further practical application, AR films with high transmittance are also required to obtain good abrasion-resistant property to extend the working life and certain hydrophobic capacity to resist the damage of humid environment.

For the advantage of easy operation and cost saving, normal sol–gel process has been widely used to produce AR films [8–10], especially in the application of covering both sides of the non-flat evacuated solar thermal glass tubes. Generally, silicon dioxide is the main material for AR films on glass surface. The silica sols can be prepared by the base or acid catalyzed processes using TEOS as precursor and the dip-coating method of silica sols on glass surface is a common way to obtain AR function [4,11,12]. Base-catalyzed sols, synthesized by the means of the typical Stöber method, usually yield to silica particle sols [13]. After both sides of the glass (refractive index n = 1.52) are coated with sols via dip-coating method, silica particles stack into films with pore structures. As a result, the refractivity can be decreased to about 1.23 and the transmittance can be obtained as high as 99%. Since only physical forces, instead of chemical bonds, exist among individual silica particles and between the particle and the glass substrate surface, the films will be irreversibly damaged even by gentle external forces [14]. Thus, the films are unable to be utilized in harsh environment and their applications are significantly limited by the poor mechanical strength. Up to now, much research has been conducted to improve the abrasion-resistance property and the mechanical strength of SiO_2-NP-composed films. Hiromitsu Kozuka published his work on preparing scratch-resistant silica particle films with high temperature post-treatment. The hardness of the films directly reached 9H after 1100 °C treatment while 6B when they were treated below 1000 °C. However, the heat treatment promoted the silanol groups over condensation, leading to a higher rank of hardness but, meanwhile, increased the refractive index [15]. Belleville deposited abrasion-resistant silica particle films strengthened

* Corresponding author. Tel./fax: +86 519 86330580.
E-mail addresses: mengxs06401320@163.com (X. Meng), wangyan1989816@126.com (Y. Wang), hnwang@cczu.edu.cn (H. Wang), zjwyz@cczu.edu.cn (J. Zhong), cxdcry@163.com (R. Chen).

0257-8972
http://dx.doi.org/10.1016/j.surfcoat.2013.10.044

by ammonia treatment at gentle temperature. Unfortunately, the treatment tended to bring about unpredictable effects on transmittance [16].

With TEOS in sol catalyzed by acid, TEOS are incompletely hydrolyzed and yield to hyrdroxyl (−OH) and residual oxyethyl (−OEt) groups, leading to linear structures with branches [14]. After coating process, with solvent volatilizing, the condensation of silanol groups (Si–OH) and residual oxyethyl groups occurs gradually and more chemical bonds form [17]. With these internal cross-linked chemical bonds and interface chemical bonds with glass substrate, acid-catalyzed films demonstrate much better scratch-resistance property, but dense structure with high refractive index [14]. Researchers have tried to mix the resultant sols respectively catalyzed by base and acid with different sol ratios to regulate film refractive index and take overall consideration of transmittance and scratch resistance [18,19]. However, because both the resultant sols had respectively completed the hydrolysis and condensation reactions before mixing, hardly any chemical bonds would generate between silica particles after mixing and the improvement in scratch resistance was still limited. Wu et al. have also published work on further strengthening the scratch resistance of porous silica films by synthesizing acid-catalyzed silica sol directly in the refluxed base-catalyzed silica sol [20]. Similarly, an inescapable trouble exits in this method: if the mole ratio of the products catalyzed by the acid to the products catalyzed by the base increases, the abrasion-resistance improves, but transmittance declines; conversely, the ratio decreases, the transmittance enhances, but the abrasion-resistance decreases.

The stability of AR films for extensive applications is also a vital aspect that should been taken into account. Usually, films prepared by sol–gel method are rich in residual silanol groups for their larger specific surface. Because of silanol groups with high surface energy, silica films usually exhibit excellent water wettability [21]. In their applications, silica AR films are easy to induce the adsorptions of water vapor and contaminants in humid surroundings. The adsorption blocks the pores in films, which results in a deterioration of the optical properties, and, thereby, the refractive index of the films increases, and the AR property deteriorates and even disappears [22]. Obviously, the outstanding wettability is not good for the applications of AR films after all, and seems to be a deadly disadvantage. Post-grafting group with low surface energy has been proposed to eliminate silanol groups so as to prevent moisture absorption and enhance the surface hydrophobicity. Organosiloxanes and fluorine organosiloxanes are usually employed to improve silica films for hydrophobicity [23–26]. Furthermore, the wettability of the silica film can be tunable by altering the surface roughness [27–29]. And, usually, the silica film with large roughness and low surface energy could reach the weak wettability. However, the overlarge roughness may also lead to light scattering which is fatal to AR effects [30].

In this paper, the multifunctional silica AR film was prepared by using base catalyzed process to obtain SiO_2-NPs first, and then by twining SiO_2-NPs with SiO_2-LPs yielded from acid catalyzed process. The introduction of the template agent further improved the film transmittance and slightly modified the film surface structures. TMCS treatment for AR film surfaces was also employed to provide films with hydrophobicity and better their durability and practicality.

2. Experimental

Fig. 1 shows the main procedure of the preparation of silica sols. During the process, TEOS was used as precursor, ammonia and hydrochloric acid as catalysts, absolute alcohol as solvent and CTAB as template agent. All the regents were analytical grade and purchased from Sinopharm Chemical Reagent Co., Ltd. (Shanghai, China).

2.1. Preparation of SiO_2-NP sol

According to Stöber method, absolute alcohol, deionized water and concentrated ammonia were first mixed. With the mixture being stirred for 5 min, TEOS was rapidly added to the mixture and stirred for 6 h at 30 °C. The final mole ratio of $EtOH:H_2O:NH_3 \cdot H_2O:TEOS$ was 37:1.2:0.8:1. The resultant sol was aged in sealed beaker at 25 °C for 3 days. The sol was then refluxed for 12 h to remove NH_3. This nanoparticle sol was coded as sol-A.

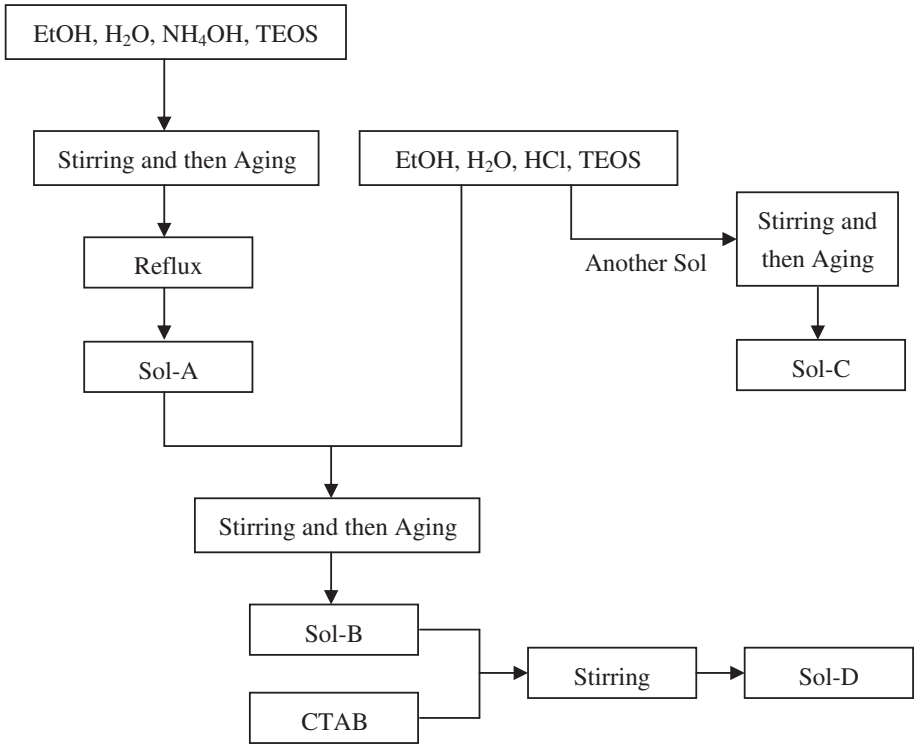

Fig. 1. The main procedure for preparation of the silica sols.

2.2. Preparation of SiO_2-LP/NP composite sol

Hydrochloric acid was first added to sol-A to generate acidic reaction condition. Then deionized water was added and stirred for 5 min. At last, TEOS were dropwise added by 30%, 50%, 60%, 70% and 80% in proportions to the total SiO_2-NPs of sol-A, assuming that 1 mol of TEOS gives 1 mol of SiO_2-NPs, respectively. The final mole ratio of HCl:H_2O:TEOS was 0.03:4:1. The new sols were stirred for 6 h at 30 °C and aged in sealed beakers at 25 °C for 5 days to allow SiO_2-LPs to grow and twine SiO_2-NPs. To make a contrast to the film from sol-A, the one-step acid catalyzed sol with the same silica concentration was also prepared, and, namely, the final molar ratio of EtOH:HCl:H_2O:TEOS was 37:0.03:4:1. The acid sols were coded as sol-B and sol-C, respectively. To introduce template agent, CTAB was added to sol-B with different molar ratio to TEOS that generated SiO_2-LPs. This templating sol was coded as sol-D.

2.3. Cleaning procedure for the substrates

The procedure for cleaning up the substrates was operated as follows: the 3 mm-thick borosilicate glass substrates (100×25 mm^2) were successively treated in basic solution and acid solution by ultrasonic for an hour. The mixed basic and acid washing solutions had the volume ratio of H_2O:H_2O_2:$NH_3 \cdot H_2O$ = 5:1:1 and H_2O:H_2O_2:HCl = 5:1:1, respectively. Then the substrates were completely cleaned up by deionized water and alcohol. Well cleaned substrates were dried off by blowing with N_2.

2.4. Dip-coating and hydrochloric modifying of AR films

All the aged sols were respectively deposited on well-cleaned substrates by the dip-coating process at a withdrawal rate of 80 mm/min. The deposited films were then dried at 75 °C for half an hour and followed by calcinations with 3 °C/min heating rate to 400 °C and insulation for 2 h in air. When the samples were cooled down naturally to ambient temperature, they were immersed in TMCS solution (10 wt.% in ethanol) for 24 h to replace the hydroxyl groups [24], and then immersed in ethanol solution for half an hour. Finally, samples were baked at 75 °C for 1 h to remove the solvent.

2.5. Characterization of silica films

The transmission spectra in the wavelength range of 400–800 nm were measured by an UV–vis spectrophotometer (Shimadzu, UV-1700). For the absence of a recognized standard for measuring the mechanical strength of the soft inorganic film [11,24], the abrasion-resistance was evaluated both by pencil hardness test and by rubbing test in this process. Water contact angles were measured by a KRŮSS instrument (Germany, DSA25). The water droplet used for the measurement was 3 μL. The surface morphologies and roughness of coated samples were characterized by atomic force microscopy (Veeco, NanoMan VS) and field emission scanning electron microscopy (CarlZeiss, SUPRA55).

3. Results and discussion

3.1. Effects of entwining structure on the property of SiO_2-LP/NP films

Fig. 2 shows the transmittance spectra in the wavelength range of 400–800 nm for films with different mole ratios of SiO_2-LPs to SiO_2-NPs on glass substrates. The average transmittance of substrate is about 91.5% in the visible wavelength range (Fig. 2a). Experimental results indicate that the film from SiO_2-NP sol catalyzed by base exhibits the best antireflective effect (Fig. 2b), while the film from SiO_2-LP sol catalyzed by acid shows the poorest (Fig. 2f). Meanwhile, the transmittance of SiO_2-LP/NP composite film decreases with the increasing mole ratio of SiO_2-LPs to SiO_2-NPs (Fig. 2c to g) and when the mole ratio is 0.8:1, the average transmittance of the composite film has almost come down as much as that of SiO_2-LP film.

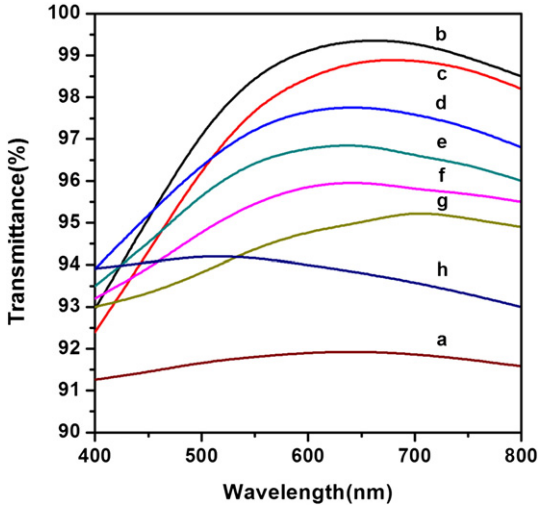

Fig. 2. Transmittances of uncoated glass (a), SiO_2-NPs film (b), film with mole ratio of SiO_2-LPs to SiO_2-NPs equals to 0.3 (c), 0.5 (d), 0.6 (e), 0.7 (f), 0.8 (g) and SiO_2-LPs film (h).

The pencil hardness test results of the films from SiO_2-NP sol, SiO_2-LP/NP composite sols and SiO_2-LP sol are shown in Table 1. Hardness test was carried out by using pencils with hardness ranging from 6B to 6H. The flat end of the pencil was placed on the film at a 45° angle to the surface with a loading of 9.8 N [31]. The first pencil that scratches the surface is reported as the hardness value, according to the ASTM Standard D 3363-00. The existence of the scratches was observed by optical microscope. As shown in Fig. 3a, scratches on the film catalyzed by the base were clearly evident even if the pencil for test was 6B, the softest pencil in this test. Therefore, the pencil hardness value of the base catalyzed film was less than 6B. With SiO_2-LPs being introduced, the hardness has obviously reached F (Fig. 3b) when the moles of SiO_2-LPs were just 30% to that of SiO_2-NPs, raising 6 grades. The hardness successively enhances with the increasing introduction of SiO_2-LPs. The hardness reached 6H when the mole ratio came to 0.7:1 (Fig. 3c), and the same hardness value indicated that its anti-abrasion property was, at least, as good as that of SiO_2-LP film. In consideration of the more loss of transmittance caused by the excessive SiO_2-LPs, the ratio 0.7:1 was selected to balance the abrasion-resistant property with the antireflective effects.

The differences of the abrasion-resistant property and antireflective effects among films from different silica sols were brought about by different structural forms of sols. Three structural forms of the above-mentioned sols and coated films can be represented as Fig. 4 shows.

In the base catalyzed process, TEOS usually yield to independent clusters, which are composed of nanoparticles without interface chemical forces. Meanwhile, these clusters sometimes bring about low specific surface, leading to fewer points to combine with glass substrate. As a result, the absence of enough combination points restraints the chances to create binding force between film and substrate. Besides, the film from SiO_2-NPs is always rich in pores and loose structures which are

Table 1
Hardness of films with different mole ratios of SiO_2-LPs to SiO_2-NPs.

SiO_2-LPs:NPs	0:1	0.3:1	0.5:1	0.6:1	0.7:1	0.8:1	1:0
Pencil hardness	<6B	F	2H	4H	6H	6H	6H

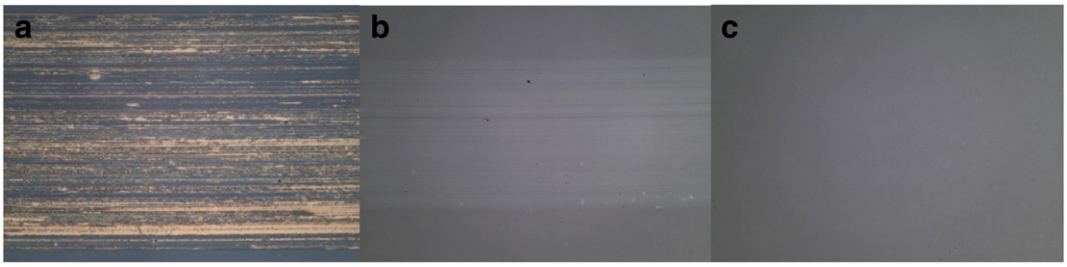

Fig. 3. Scratches for SiO_2-NPs film (a) with 6B pencil; 30% SiO_2-LPs film (b) with F pencil and 70% SiO_2-LPs film (c) with 6H pencil (magnified by 40 times).

also negative for abrasion-resistant property. However, according to Eq. (1):

$$n_{pc}^2 = \left(n_{dc}^2 - 1\right)(1 - P/100) \quad (1)$$

in which n_{pc} and n_{dc} are the refractive index of the porous and dense silica coating respectively and P is the percentage of porosity, and the increase of P would effectively lower the refractive index and enhance the transmittance of films [32,33]. Thus, films from SiO_2-NPs tend to demonstrate good AR functions. Distinct from base catalyzed process, acid catalyzed process usually generates linear silica polymers with smaller sizes, which easily give rise to chemical bonds condensation between silica film and glass substrate because of larger contact area and active residual oxyethyl groups of polymers. Meanwhile, the way of polymers combination among themselves gives the film strong internal cross-linked chemical bonds, providing extremely dense structure but high refractive index and poor AR effects. Surprisingly, twining SiO_2-NPs from sol catalyzed by base process with SiO_2-LPs catalyzed by acid process can both obtain solid structure and remain certain porosity simultaneously. This method that catalyzes TEOS in nanoparticle sol under acidic circumstance to create chain and sphere structures with chemical bonds would effectively enhance the abrasion-resistance property of the film from SiO_2-NPs. Besides, the existence of SiO_2-NPs always leaves the chance to produce pore structures. Thus, the film from SiO_2-LP/NP composite sol shows good adhesive property and retains certain AR effects concurrently.

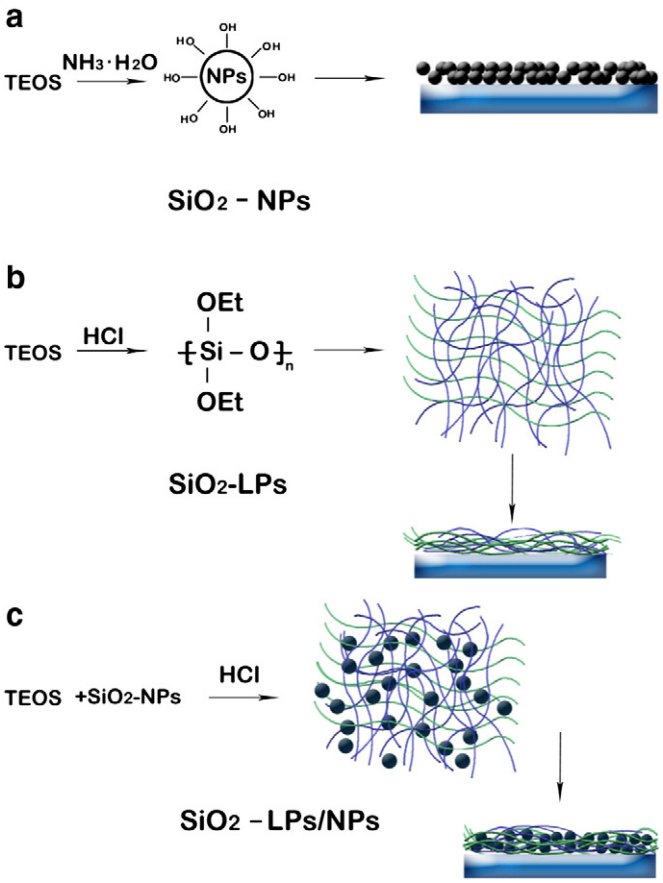

Fig. 4. Schematic diagram of film forming process from SiO_2-NPs (a), SiO_2-LPs (b), and SiO_2-LPs/NPs composite sol (c).

3.2. Effects of template agent on transmittance and abrasion-resistance property of SiO_2-LP/NP composite AR films

SiO_2-LP/NP film with 0.7:1 mol ratio of SiO_2-LPs to SiO_2-NPs has obtained excellent abrasion-resistance property, but its average transmittance is only 95.2%, as shown in Fig. 5b. The increase of average transmittance is always proportional to the porosity of film when the film thickness is fixed in about a quarter of the incident light wavelength, according to Eq. (1). Although it is available to increase the content of SiO_2-NPs in composite film to enrich pore structures, their abrasion-resistance declines seriously. However, template agent introduction is a masterly and feasible method to construct pore structures by occupying the space during the sol–gel coating process and then be removed by heat treatment [31]. Consequently, CTAB was used as pore-forming agent successfully in this study. The experimental results indicated that the transmittance had obviously increased when CTAB introduced was just 6% the mole of SiO_2-LPs (Fig. 5c). Meanwhile, antireflective effects were promoted step by step with the increase of template agent (Fig. 5d, e). However, excessive CTAB addition, 18% of the mole of SiO_2-LPs, led to excessive porosity and declining the ordering

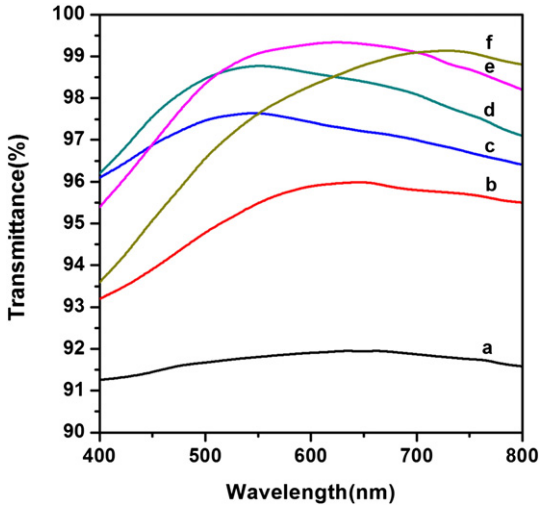

Fig. 5. Transmittances of uncoated glass (a) and film with different mole ratio of CTAB to SiO_2-LPs, 0:1 (b), 0.06:1 (c), 0.12:1 (d), 0.15:1 (e) and 0.18:1 (f).

of the pore structure, which brought about light scattering and the deterioration of AR effects (Fig. 5f). Therefore, according to the results of the experiment, 12% of the mole of SiO_2-LPs is the best ratio to improve transmittance for SiO_2-LP/NP composite film and the peak and the average transmittance are 99.3% at 620 nm and 98.4% respectively. The average transmittance increases by 3.2% compared with the composite film without any CTAB introduction and increases by 7% compared with bare glass substrate, displaying remarkable AR effects.

The porous composite film with CTAB introduction which exhibited best transmittance was tested by pencil hardness tester in the same way. The test result shows its hardness is 5H, with one rank lower to the film before template introduction. This may be caused by the slightly loosened structure resulting from new pore structures created by CTAB. To get further indication of the film abrasion-resistance, the rubbing test was also conducted. For the rubbing test, namely, rub the coating 100 times with cotton balls immersed with some ethanol and dust; and, then, compare the transmittance spectra before and after rubbing. Fig. 6a demonstrates the transmittance spectra before and after 100 times rubbing. The composite film before CTAB introduction, for the contrast of the whole transmittance spectra in the wavelength range of 400–800 nm, was also evaluated through rubbing test, as shown in Fig. 6b. Both of the transmittances of the porous composite film and the composite film decreased just a little, undoubtedly, the result of rubbing test corresponds to that of the hardness test. Furthermore, the porous composite film with much higher transmittance is rather in noticeable.

3.3. Relationships of surface morphologies with the abrasion-resistance property and hydrophobicity of AR films

The surface morphology was characterized by atomic force microscopy (AFM). Different surface morphology images for films are shown in Fig. 7. The film from simple SiO_2-NP sol appears with loose structure and concave–convex morphology (Fig. 7a). The appearance may be determined by the stack of massive SiO_2-NP clusters that were generated in the solvent evaporation process of coating procedure. For lacking of strong chemical bonds between clusters or nanoparticles, the film from base catalyzed silica sol shows extremely poor abrasion-resistance property. While in acid catalyzed process, the growth of the polysilicates turns out to be linear polymers with smaller granular sizes. The film from simple SiO_2-LP sol appears extremely dense and smooth with no fluctuations or uneven structures (Fig. 7d). The surface morphology feature of SiO_2-LP/NP composite film is a comprehensive

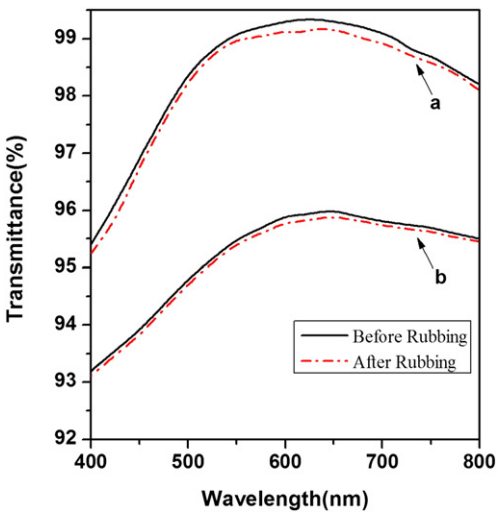

Fig. 6. Transmittance of the porous SiO_2-LPs/NPs film (a) and the SiO_2-LPs/NPs composite film (b) before and after rubbing.

suite of SiO_2-NPs and SiO_2-LPs (Fig. 7b). It is unexpected that the abrasion-resistance property of composite film is more inclined to that of the film from SiO_2-LPs. For SiO_2-LP/NP composite sol, the twining mode, on one hand, strengthens the binding forces between two forms of silica by strong chemical bonds, instead of weak physical bonds; on the other hand, the chain and sphere structure creates after twining and condensation of silanol groups, which prevents the existence of SiO_2-NP clusters or nanoparticles from being greatly raised on the surface. The combination of SiO_2-LPs and SiO_2-NPs tends to make the surfaces of composite AR films tend to be a little smooth and homogeneous, which benefits the improvement in abrasion-resistance property.

To further explore the evidences of above inferred reasons for great improvement in abrasion-resistance property after the introduction of SiO_2-LPs to SiO_2-NPs, FESEM instrument was also employed to characterize the surface and cross section morphologies of films before and after SiO_2-LPs introduction, as shown in Fig. 8. The surface for SiO_2-LP/NP composite film was obviously denser than that of SiO_2-NPs, which means the dense SiO_2-LPs had filled up the film and fastened the silica nanoparticles with the film. Furthermore, the silica clusters almost disappeared according to the observation of the cross section morphologies after and before SiO_2-LPs introduction. The disappearance of silica clusters may be caused by different feed methods in the synthesizing process of composite sol. The composite sol, prepared by directly adding TEOS to acidic SiO_2-NP sol rather than simply mixing the resultant SiO_2-LP sol and SiO_2-NP sol, greatly reduced the chance of the generation of clusters from silica nanoparticles. Usually, the cross section morphology can stand for the inner structure of film, to some extent. Therefore, the results of FESEM tests could well correspond to that of AFM analysis.

In general, the pore size of porous silica film, deriving from the sol–gel process by using CTAB as template agent, ranges from 2 to 3 nm [34]. As shown in Fig. 7c, the morphology of porous composite film with template agent introduction does not appear to have any variations compared with Fig. 7b. The small pore size seemed little affecting on the integral structure and maintained the abrasion-resistance property of SiO_2-LP/NP composite film, for which, the pencil hardness was 5H.

Although aforementioned porous composite film has been equipped with both AR effects and abrasion-resistance, it also needs to possess good hydrophobicity to resist the penetration of water vapor and the adsorption of contaminants in the air to preserve the stable AR effects for longer. Usually, the hydrophobic nature of the coating surface can be quantified by measuring the contact angle of water droplet (WCA) with the surface [35]. For SiO_2-NP film, WCA before TMCS treatment was just 6°, a super-hydrophilicity surface. WCA measuring results of different films after TMCS treatment are listed in Table 2. The data reveal that WCAs of SiO_2-NP films after TMCS treatment rose to 126°, indicating a significant increase in hydrophobicity. However, WCA of TMCS treated film from SiO_2-LPs was merely 62°. The big difference of hydrophobicity between the above two films is closely related to the roughness, and the value of roughness is determined by the surface morphology of the film. As shown in Fig. 7a, the concave–convex morphology of SiO_2-NP film piled up by nanoparticle clusters constructed the roughness, and the Rq value was as high as 6.26 nm. While the surfaces for SiO_2-LP/NP composite films before and after CTAB introduction become a bit smoother, of which Rq decreased to 2.96 and 3.31 nm, respectively, the rough concave–convex morphologies had been well preserved and WCAs were almost as high as that of SiO_2-NP film. Besides, with the introduction of CTAB, the Rmax value of the porous composite film decreased from 35.5 nm to 30.5 nm, a decrease in the height of peak to valley. Meanwhile, the new produced pores roughed the composite film surface and increased the value of Rq from 2.96 nm to 3.31 nm and Ra from 2.34 nm to 2.63 nm. Thus, it may be concluded that the introduction of the template CTAB assuaged the clusters with relatively large sizes and improved the roughness by abundant mesoporous with relatively small sizes. The former was beneficial to abrasion-resistance, while the later

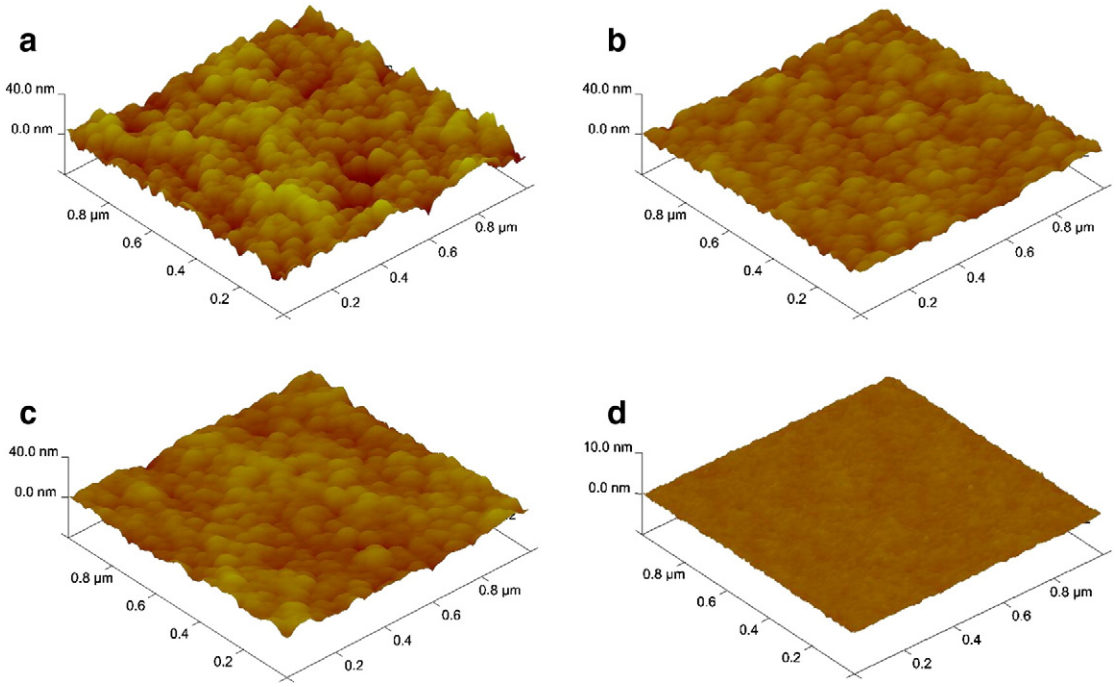

Fig. 7. Images of 3D-AFM morphologies of SiO_2-NPs film (a); SiO_2-LPs/NPs film (b), porous SiO_2-LPs/NPs film (c) and SiO_2-LPs film (d).

was beneficial to hydrophobicity. As for SiO_2-LP film, the surface is extremely dense and smooth and its Rq value was just 0.230 nm, which certainly leads extremely poor hydrophobicity. In summary, the films from the sols that contain silica nanoparticles tend to have large WCA because of the relatively large roughness of the surface, which promoted by the particle cumulate structures formed in the coating process.

4. Conclusions

A composite silica sol was prepared by the acid catalyzed process operated in silica nanoparticle sol. This procedure promoted the formation of twining structures by chemical bonds between SiO_2-LPs in acid catalyzed process and SiO_2-NPs in base catalyzed process. The generation of SiO_2-LPs dramatically enhanced the abrasion-resistance property of SiO_2-NP film greatly. The introduction of template agent CTAB into SiO_2-LP/NP composite sol could further improve the AR effects of the abrasion-resistant composite film. The porous composite film with ratios of n_{LP}:n_{NPs} = 0.7:1 and n_{CTAB}:n_{LPs} = 0.15:1 exhibits excellent AR effects with 99.3% peak and 98.4% average transmittance. The pencil hardness of the film also reaches 5H and only a little transmittance decline occurs after 100 times rubbing, displaying remarkable abrasion-resistance property. TMCS treatment is proved to be a feasible way to

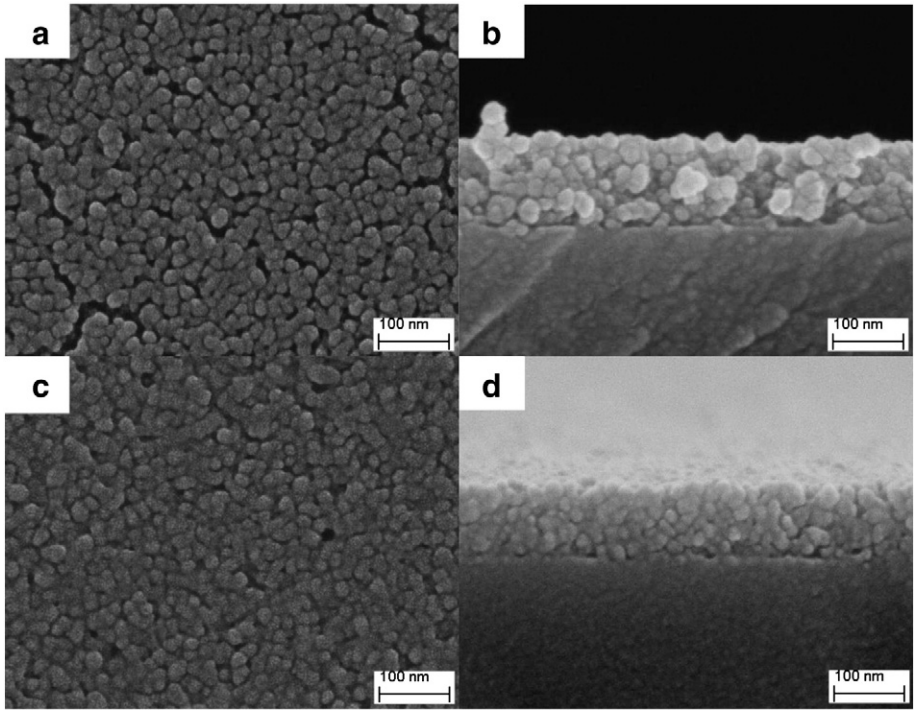

Fig. 8. FESEM surface images of SiO_2-NPs film (a) and SiO_2-LPs/NPs film (c). Cross section morphologies of SiO_2-NPs film (b) and SiO_2-LPs/NPs film (d).

Table 2
Roughness parameters and WCA of different films treated by TMCS.

	SiO_2-NP film	SiO_2-LP/NP film	Porous SiO_2-LP/NP film	SiO_2-LP film
Rq (nm)	6.26	2.96	3.31	0.230
Ra (nm)	4.96	2.34	2.63	0.182
Rmax (nm)	50.3	35.5	30.5	2.97
WCA (°)	126	118	120	62

Where Rq is the root mean square (RMS) roughness, the most widely used amplitude roughness parameter; Ra is the mean deviation of height; Rmax is the height of peak to valley.

alter the hydrophobicity of the objective film from 6° to 120° and enhance the stability. All the results have proved that the multiple performances would well meet the needs of practical application in wild harsh environments.

Acknowledgments

The authors acknowledge the financial support of the Project funded by the Priority Academic Program Development of Jiangsu Higher Education Institutions, the Project supported by National Science Foundation of China (Grant No. 21101017/B0107) and the program granted by the Innovation Project of Postgraduates in Jiangsu Province (CXZZ11-0376).

References

[1] K. Abe, Y. Sanada, T. Morimoto, J. Sol-Gel Sci. Technol. 22 (2001) 151.
[2] P. Belleville, P. Prené, F. Mennechez, C. Bouigeon, Proc. SPIE 4804 (2002) 69.
[3] Y. Xu, B. Zhang, W.H. Fan, D. Wu, Y.H. Sun, Thin Solid Films 440 (2003) 180.
[4] M.C. Bautista, A. Morales, Sol. Energy Mater. Sol. Cells 80 (2003) 217.
[5] P. Nostell, A. Roos, B. Karlsson, Thin Solid Films 351 (1999) 170.
[6] G. Helsch, A. Mös, J. Deubener, M. Höland, Sol. Energy Mater. Sol. Cells 94 (2010) 2191.
[7] I. Bita, T. Choi, M.E. Walsh, H.I. Smith, E.L. Thomas, Adv. Mater. 19 (2007) 1403.
[8] D.R. Uhlmann, T. Suratwala, K. Davidson, J.M. Boulton, G. Teowee, J. Non-Cryst. Solids 218 (1997) 113.
[9] Y.H. Xiu, F. Xiao, D.W. Hess, C.P. Wong, Thin Solid Films 517 (2009) 1610.
[10] M. Manca, A. Cannavale, L.D. Marco, A.S. Aricò, R. Cingolani, G. Gigli, Langmuir 25 (2009) 6357.
[11] S.I. Huang, Y.J. Shen, H. Chen, Appl. Surf. Sci. 255 (2009) 7040.
[12] H.K. Raut, A.S. Nair, S.S. Dinachali, V.A. Ganesh, T.M. Walsh, S. Ramakrishna, Sol. Energy Mater. Sol. Cells 111 (2013) 9.
[13] W. Stöber, A. Fink, E. Bohn, J. Colloid Interface Sci. 26 (1968) 62.
[14] F.T. Chi, L.H. Yan, H.B. Lv, B. Jiang, Mater. Lett. 65 (2011) 1095.
[15] H. Kozuka, A. Yamano, M. Fujita, H. Uchiyama, J. Sol-Gel Sci. Technol. 61 (2012) 381.
[16] P.F. Belleville, H.G. Floch, Proc. SPIE 2288 (1994) 25.
[17] A. Mehner, J. Dong, T. Prenzel, W. Datchary, D.A. Lucca, J. Sol-Gel Sci. Technol. 54 (2010) 355.
[18] G.M. Wu, J. Wang, J. Shen, T.H. Yang, Q.Y. Zhang, B. Zhou, Z.S. Deng, B. Fan, D.P. Zhou, F.S. Zhang, Mater. Sci. Eng. B 78 (2000) 135.
[19] Y.Q. Xiao, J. Shen, Z.Y. Xie, B. Zhou, G.M. Wu, J. Mater. Sci. Technol. 23 (2007) 504.
[20] G.M. Wu, J. Wang, J. Shen, Q.Y. Zhang, B. Zhou, Z.S. Deng, B. Fan, D.P. Zhou, F.S. Zhang, J. Phys. D. Appl. Phys. 34 (2001) 1301.
[21] J. Yang, J. Chen, J.H. Song, Vib. Spectrosc. 50 (2009) 178.
[22] G.S. Vicente, R. Bayón, N. Germán, A. Morales, Sol. Energy 85 (2011) 676.
[23] Q.P. Ke, W.Q. Fu, S. Wang, T.D. Tang, J.F. Zhang, ACS Appl. Mater. Interfaces 2 (2010) 2393.
[24] X.G. Li, J. Shen, Thin Solid Films 519 (2011) 6236.
[25] D. Goswami, S.K. Medda, G. De, ACS Appl. Mater. Interfaces 3 (2011) 3440.
[26] O. Nimittrakoolchai, S. Supothina, J. Eur. Ceram. Soc. 28 (2008) 947.
[27] Y. Li, W.P. Cai, B.Q. Cao, G.T. Duan, F.Q. Sun, C.C. Li, L.C. Jia, Nanotechnology 17 (2006) 238.
[28] S. Pilotek, H.K. Schmidt, J. Sol-Gel Sci. Technol. 26 (2003) 789.
[29] H. Yang, X.J. Zhan, Z.Q. Cai, P.H. Pi, D.F. Zheng, Surf. Coat. Technol. 205 (2011) 5387.
[30] Y. Li, F. Liu, J.Q. Sun, Chem. Commun. 19 (2009) 2730.
[31] W. Joo, Y. Kim, S.J.K. Kim, Thin Solid Films 519 (2011) 3804.
[32] B.E. Yoldas, Appl. Opt. 19 (1980) 1425.
[33] B.E. Yoldas, D.P. Partlow, Thin Solid Films 129 (1985) 1.
[34] B.G. Kum, Y.C. Park, Y.J. Chang, J.Y. Jeon, H.M. Jang, Thin Solid Films 519 (2011) 3778.
[35] S.S. Latthe, H. Imai, V. Ganesan, A.V. Rao, Microporous Mesoporous Mater. 130 (2010) 115.